



Particle shape accounts for instrumental discrepancy in ice core dust size distributions

Marius Folden Simonsen¹, Llorenç Cremonesi², Giovanni Bacco⁴, Samuel Bosch¹, Barbara Delmonte⁴, Tobias Erhardt³, Helle Astrid Kjær¹, Marco Potenza², Anders Svensson¹, and Paul Vallelonga¹

¹Centre for Ice and Climate, Niels Bohr Institute, University of Copenhagen, Copenhagen, Denmark

²Department of Physics, University of Milan and National Institute for Nuclear Physics (INFN), Via Celoria 16, I20133 Milan, Italy

³Climate and Environmental Physics, Physics Institute & Oeschger Centre for Climate Change Research, University of Bern, Sidlerstrasse 5, 3012 Bern, Switzerland

⁴Department of Earth and Environmental Sciences, University Milano-Bicocca, Piazza della Scienza 1, I20126 Milan, Italy

Correspondence to: Marius Folden Simonsen (msimonse@fys.ku.dk)

Abstract. The Klotz Abakus laser sensor and the Coulter Counter are both used for measuring the size distribution of insoluble mineral dust particles in ice cores. While the Coulter Counter measures particle volume accurately, the equivalent Abakus instrument measurement deviates substantially from the Coulter Counter depending on the type of sample. We show that the difference between the Abakus and the Coulter Counter measurements is mainly caused by the irregular shape of dust particles in ice core samples. The irregular shape leads means that the calibration routine based on standard spheres must be adjusted. This new calibration routine gives an increased accuracy on Abakus measurements, which may improve future ice core record intercomparisons. We derived an analytical model for extracting the aspect ratio of dust particles from the difference between Abakus and Coulter Counter data. For verification, we measured the aspect ratio of the same samples directly using a Single Particle Extinction and Scattering Instrument. The results demonstrate that the model is accurate enough to discern between samples of aspect ratio 0.3 and 0.4 using only the comparison of Abakus and Coulter Counter data.

1 Introduction

Ice cores from Greenland contain a record of climate proxies over the last 120,000 years. One of those proxies is mineral dust in the size range 0.5-100 μm . The dust has several properties that all give useful information of the past: concentration, size distribution, morphology and chemical and isotopic composition. These measurements have revealed that the dust in ice cores come from central Asia during both the Holocene and the last glacial period (Biscaye et al., 1997). The observed 100 times decrease in dust concentration from glacial to Holocene has constrained the aridity, windiness and insolation forcing of glacial climate models (Ruth et al., 2003; Steffensen, 1997).

Traditionally, the Coulter Counter technique has been used to measure concentration and size distribution. It works by measuring the electrical impedance over an orifice, through which a sample flows.

For ice cores, this sample is melted ice core water, with pure NaCl added to stabilise the electrical conductivity. When a particle flows through and displaces the conductive liquid, the impedance rises. This signal increases with the particle volume. The



Coulter Counter has the disadvantage that it applies only to discrete samples and cannot be easily combined with continuous flow analysis (CFA) systems (Röthlisberger et al., 2000; Kaufmann et al., 2008) due to its sensitivity to electrical noise.

CFA systems on the other hand are a common technique for preparing ice core samples for impurity analysis, offering greater measurement speed and often higher resolution. On the Copenhagen CFA system, $35 \times 35 \times 550$ mm sticks are cut from the ice core and melted standing on a gold coated melt head (Bigler et al., 2011). The melt water from the outer 5 mm of the ice core surface is discarded, while the inner uncontaminated water is transported by a peristaltic pump to the connected instruments. One of these instruments is the Abakus laser sensor (LDS23/25bs, Klotz GmbH, Germany) for measuring insoluble particle concentration and size distribution.

The Abakus instrument measures the intensity of laser light shone through a flow cell where the sample liquid flows through. When a particle passes, the light is attenuated. The Abakus therefore measures the optical extinction cross section of the particle. It can measure particles in the range 1-15 μm . Since it measures optical transmissivity rather than electrical impedance, it is much less sensitive to electrical noise than the Coulter Counter. The Abakus on a CFA system can have a measurement depth resolution of 3 mm (Bigler et al., 2011), and requires almost no maintenance when the CFA system is running. The Coulter Counter on the other hand typically integrates a thicker interval, and requires work from the operator all the time during measurements (Delmonte et al., 2004; Lambert et al., 2012).

The aspect ratio of ice core dust particles was measured using the novel Single Particle Extinction and Scattering (SPES) instrument (Villa et al., 2016; Potenza et al., 2016). In addition to the extinction cross section, which is also measured by the Abakus, it measures the optical thickness of the particles (Potenza et al., 2016). The optical thickness depends on the geometrical thickness of the particle and its refractive index. If the refractive index is known, the aspect ratio can be derived from the combination of extinction cross section and geometrical thickness. The SPES is able to discern between oblate and prolate particles.

The extinction and scattering cross sections of irregularly shaped particles can be accurately calculated with the discrete dipole approximation (DDA) (Draine and Flatau, 1994). In the present work, we have used the Amsterdam Discrete Dipole Approximation (ADDA) code (Yurkin and Hoekstra, 2011). The ADDA simulations were used to simulate the SPES measurements and thereby extract the aspect ratio from the SPES data. Furthermore it was used to show that the Mie scattering wiggles effects on the optical extinction cross section seen for spherical particles cancel out for ice core dust due to its irregular shape (Chýlek and Klett, 1991).

The measured samples are from the Renland Ice Cap Project (RECAP) ice core that was drilled during the summer of 2015 on the Renland ice cap in Eastern Greenland only 2 km away from the old Renland ice core (Hansson, 1994). This ice core covers the last glacial cycle, and samples were taken from both the Holocene and the last glacial period (supplement A). As found for the central Greenlandic ice cores, the glacial RECAP dust comes from central Asia (Biscaye et al., 1997). However, the Holocene dust, like in the old Renland core (Bory et al., 2003), is dominated by a local East Greenlandic source (Bory et al., 2003). The volume mode of the glacial dust is 2 μm , while it is 20 μm for the Holocene dust, due to the increased transport induced size fractionation for the glacial dust (Ruth et al., 2003).

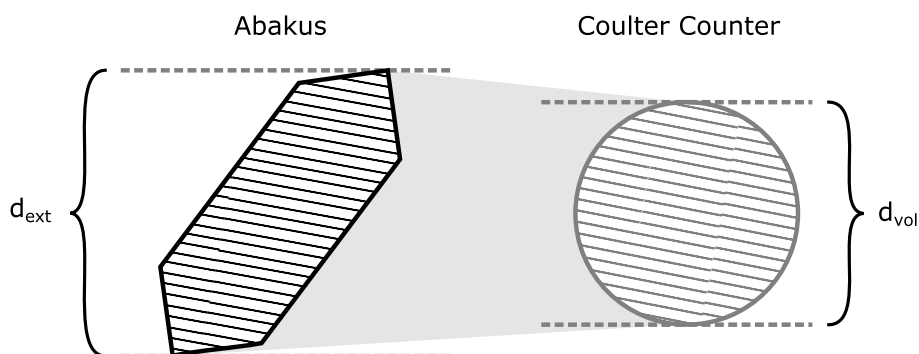


Figure 1. The Abakus measures the extinction cross section of the particles, while the Coulter Counter measures their volume. Both instruments convert this to an equivalent diameter, d_{ext} and d_{vol} respectively.

Although both instruments are typically calibrated using standard spheres of known diameter, they produce substantially different size distribution results when ice core samples are measured (Ruth et al., 2003; Lambert et al., 2008, 2012; Koffman et al., 2014). It has been proposed that this difference is because ice core dust is generally non-spherical (Lambert et al., 2012; Potenza et al., 2016). and we show here that the non-spherical shape of the particles does quantitatively account for the main discrepancy between the two instruments (Figure 1). One important shape effect arises from the aspect ratio, defined as the ratio between the length of its shortest and the longest side. To distinguish between oblate and prolate particles, we use aspect ratios less than 1 for oblates and larger than 1 for prolates. We have measured the aspect ratio of Greenland ice core dust particles to be 0.3 – 0.4, which is significantly different from the aspect ratio of 1 of the polystyrene standard spheres used for calibration. Since our results are valid both for large mode local East Greenlandic and small mode distant East Asian dust, we expect that they can be generalized to other ice cores.

2 Materials and Methods

2.1 Abakus

For the Abakus measurements, square sticks of $35 \times 35 \times 550$ mm were cut from the center of the RECAP ice core, These sticks were melted on the RECAP CFA system. This CFA system is an enlargement of the one described by Bigler et al. (2011), with greater melt rate, more analytical channels and pressure decoupling after the debubbler. The Abakus was connected to the CFA system, and had a flow rate of 2 mL/min. The attached tubes and the Abakus were cleaned with MQ water (Millipore Advantage, 18.2 MOhm/cm) after each 5.5 m of ice measured during the measurement campaign. Occasionally the Abakus was clogged by a large particle and needed flushing with a syringe while the system was running. The depth resolution is 5 mm due to mixing in the tubes from the melt head to the Abakus. The Abakus was originally calibrated to give the correct diameter for polystyrene beads of 2, 5, and 10 μm .



Polystyrene standard spheres 1.5, 2, 4, 5 and 10 μm diameter from BS-Partikel GmbH, Wiesbaden, Germany (supplement B), were measured by the Abakus. They were diluted to concentrations between 15000 and 90000 particles/mL. To avoid coagulation, the standards were sonicated for 30 seconds before measurements. Each of the standards was measured for 6 minutes. They were stored upright in a refrigerator between measurements.

5 2.2 Coulter Counter

The Coulter Counter measured samples of 55 cm length. The measured ice was an outer ice core triangular piece of 3×1 cm cross section that was broken into smaller pieces of 10 cm. The samples were decontaminated by rinsing in three consecutive jars of MQ water. In each jar the outer layer of ice was melted away and removed, leaving only the cleaner inner part to be analyzed. This treatment reduced the sample size by 50%. The samples were measured in two Beckman Coulter Counters, one with a 100 μm aperture and one with a 30 μm aperture. The samples were shaken before being measured by the 100 μm Coulter Counter, which took around 2 minutes. Afterwards the samples were measured by the 30 μm Coulter Counter. The 30 μm aperture data were used for particles smaller than 4 μm and the 100 μm aperture data were used for particles larger than 4 μm . Only selected samples, representative of Holocene and glacial climates, were measured by the Coulter Counter. For the Holocene, selected samples from 356 to 4008 years b2k (before AD 2000) were used, while for the glacial, the whole period from 17760 to 33885 years b2k was measured (supplement A). The same samples were used for the Abakus.

2.3 SPES

After the Coulter Counter measurements, the samples were measured by SPES (section 3.3). The sample flows through a 200 μm flow cell, and is illuminated by a laser. The light is measured by two detectors, which in combination gives the extinction cross section and the optical thickness. There is no focusing of the particle stream in the cell, so only a small fraction of the particles passing through the cell is measured by the laser. Therefore the sample is circulated through the cell several hundred to thousand times. This gives an accurate measure of the shape distribution of the particles, but it does not allow concentration measurements.

The narrow cell ensures high shear, forcing the particles to attain a preferential direction along one direction. Oblate particles in a shear flow orient themselves with the flat side along the flow lines, and are randomly oriented in the shear direction. Prolates lie in a plane of constant velocity, and are free to rotate within it (Jeffery, 1922).

3 Results

3.1 ADDA simulations

Using the Amsterdam Discrete Dipole Approximation software (ADDA), we have calculated the extinction diameter for different particles. For spherical particles much larger than the wavelength of the light, the relation between diameter and optical extinction cross section is $\sigma_{\text{ext}} = \frac{\pi}{2}d^2$. For smaller particles of size comparable to the light wavelength, the relation differs due



to optical effects (Figure 2) (van de Hulst, 1957). However, we define the extinction diameter as $d_{\text{ext}} = \sqrt{\frac{2}{\pi} \sigma_{\text{ext}}}$ for all particles. Besides, we associate each particle with its volumetric diameter: A sphere with volume V has the diameter $d_{\text{vol}} = \sqrt[3]{\frac{6V}{\pi}}$. For any particle of known volume, the volumetric diameter is given by this relation.

Specifically, we have used ellipsoids and oblate prisms with an aspect ratio of 0.3 in the volumetric diameter range 1 to 8 μm (Figure 3). While spheres have a unique extinction diameter for each volume diameter, the extinction diameter of other particles depends on their orientation. For each volumetric diameter, there will therefore be a probability density function of extinction diameter. When the Abakus measures a particle, it gives a specific extinction diameter with a probability given by this probability density function. The broadness of the probability density function for non-spherical particles means that the wiggle pattern is smeared out. Furthermore, the wiggles are not located at the same d_{vol} for different particle shapes. Since ice core dust has a variable shape (supplement C), it is sampled from a sum of the ellipsoid, prismatic and many more distributions. In this sum of distributions the wiggles average out.

The average extinction diameter is higher than the volumetric diameter. This is because the particles are elongated, as will be shown in section 3.4. For particles larger than 1.7 μm , the average extinction diameter is approximately proportional to the volumetric diameter. For much smaller particles, the extinction diameter is independent of the particle shape. The Abakus after calibration (section 3.2) does however not measure particles smaller than 1.8 μm , so the measured Abakus data is within the range of proportionality: $d_{\text{ext}} \propto d_{\text{vol}}$.

3.2 Particle size standard calibration

We have measured the size of five different particle size standards (supplement B, section 2.1) with the Abakus (Figure 2). The 2, 5, and 10 μm standards were measured twice with a one year delay, without significantly different results. This shows that the Abakus calibration is stable over the time scale of a typical measurement campaign.

Since d_{ext} is proportional to d_{vol} for ice core dust (section 3.1), and the proportionality constant depends on particle shape and is unknown, we would like to calibrate the Abakus such that it gives the extinction diameter d_{ext} and not the true diameter for the standard spheres (using the term true for the certified diameter given by the manufacturer). Therefore we define a calibration function such that the measured diameter divided by the calibration function is the extinction diameter. To avoid artifacts in the calibrated distribution, the calibration function has to be a continuous function of the measured diameter with a continuous first derivative. Since we want the relative error on each standard to have the same weight, the function is fitted to the logarithm of the ratio between the measured and extinction diameter. The function $y = a(x - x_0)^2$, where $y = \frac{\ln(d_{\text{meas}})}{\ln(d_{\text{ext}})}$ and $x = \ln(d_{\text{meas}})$, is fitted to the data as calibration function (Figure 4). The fit parameters found are $(a, x_0) = (-0.086, 2.60)$. This particular calibration function is chosen because it is simple, fits the data well and satisfies the conditions described above. $x_0 = 2.60$ corresponds to $d_{\text{meas}} = 13.5 \mu\text{m}$. As the calibration function is equal to 1 for $d_{\text{meas}} = 13.5 \mu\text{m}$ and standards larger than 13.5 μm were not tested, no calibration is applied for diameters larger than 13.5 μm .

The particle size standard calibration has been applied to ice core dust data (Figure 5). Since the calibration function is less than 1 for diameters smaller than 13.5 μm , the effect of applying the calibration function is that the small diameter data is

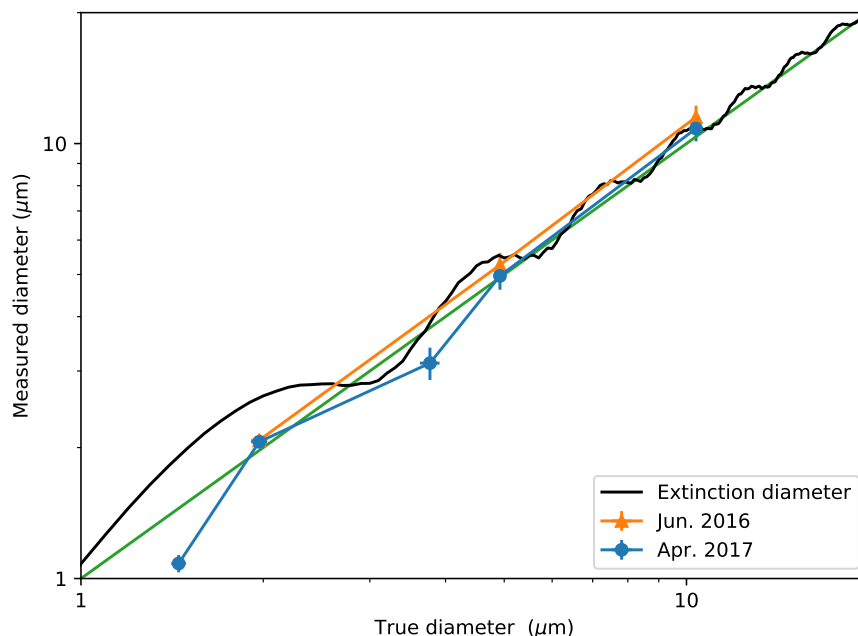


Figure 2. The blue circles are the diameter of standard polystyrene spheres measured by the Abakus as a function of the true diameter certified by the manufacturer. The orange triangles are three of the same standards measured a year earlier. The black curve is the optical extinction diameter of a sphere as a function of diameter. The green line is where the measured and the true diameter are equal, to which the extinction diameter converges for large true diameters.

shifted towards larger diameters. This is most pronounced for the smallest diameters, since the calibration values are smallest for small diameters. The positive slope of the calibration function means that the calibrated bin positions are squeezed more tightly together than the uncalibrated bins. Since the probability density function is defined as the number of counts in a bin divided by its size, the calibrated probability density function has higher values than the uncalibrated one. This effect decreases with diameter, as the slope decreases.

3.3 SPES

We have measured optical thickness (ρ) and extinction cross section (σ_{ext}) with SPES for both Holocene and glacial samples (Figure 6). By comparing to ADDA simulations, it was found that the samples are dominated by oblates (Villa et al., 2016). The distribution of particles in $\rho, \sigma_{\text{ext}}$ space can be simulated using ADDA for a given particle shape and size distribution.

10 We have done this for several different volumetric diameter size distribution and oblate right square prisms of aspect ratios 0.2, 0.25, 0.3, 0.4 and 0.5. To compare the simulations and the data, first the average of the logarithm of the simulated optical thickness as function of extinction cross section was calculated. This was used as fit function for a least squares fit to the measured data, where the parameter varied in the fit was the aspect ratio. As the refractive index of ice core dust is between

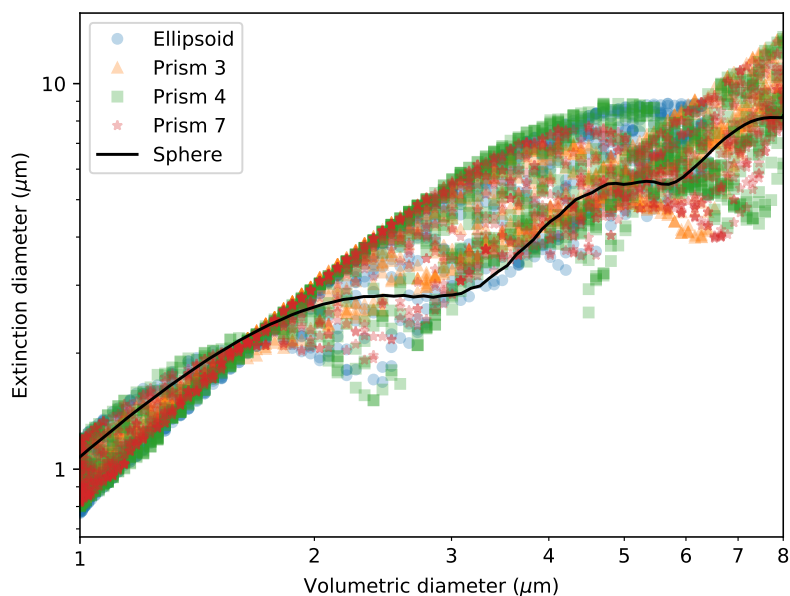


Figure 3. ADDA simulations of particles with a refractive index of 1.586 and, except for the spheres, an aspect ratio of 0.3. The prisms are oblate and their cross sections are equilateral polygons with 3, 4 and 7 sides.

1.52 and 1.55 (Royer et al., 1983), we have run the simulations using these two limiting refractive indices. The result did not depend significantly on the volumetric diameter size distribution used in the simulation. For $n = 1.52$ the Holocene aspect ratio is 0.42 ± 0.03 and the glacial is 0.38 ± 0.02 , while for $n = 1.55$ the Holocene is 0.36 ± 0.01 and the glacial is 0.29 ± 0.01 . The uncertainties arise from the parabolic fit. The average in the refractive index range of ice core dust is therefore 0.39 ± 0.03 for the Holocene and 0.33 ± 0.04 for the glacial.

For low and high extinction cross sections, the SPES is not sensitive in the full optical thickness range. This would give a bias when fitting to the simulated data. Therefore, only data between the 0.25 and 0.75 quantile of the extinction cross section was used.

3.4 Aspect ratio effect

Spheres have the lowest geometrical cross section to volume of all particles, when averaged over all rotation angles of the particles (Brazitikos et al., 2014). Let us for a particle define the geometric cross section diameter as $d_{\text{geom}} = \sqrt{\frac{2}{\pi} \sigma_{\text{geom}}}$, where σ_{geom} is the geometric cross section of the particle. However, since ice core dust is non-spherical, (section 3.3), $d_{\text{geom}} > d_{\text{vol}}$ and $d_{\text{ext}} = d_{\text{geom}}$ (section 3.2). We can therefore calculate the distribution of d_{ext} based on the aspect ratio c and the distribution of d_{vol} . The distribution of d_{vol} , $\frac{dP(d_{\text{vol}})}{d \ln d_{\text{vol}}}$, can be determined by the Coulter Counter.

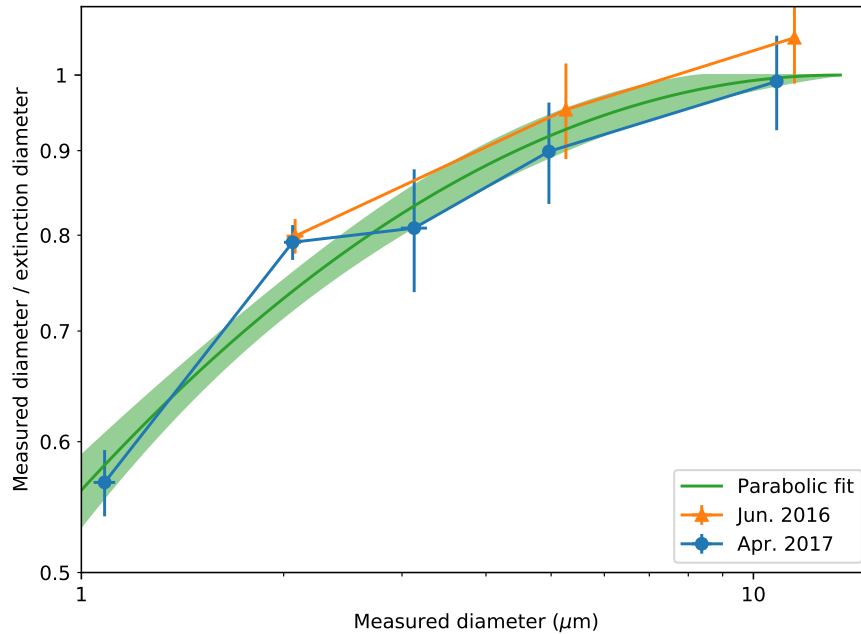


Figure 4. The blue circles are the ratio between the diameter of spheres measured by the Abakus and their extinction diameter (figure 2). The orange triangles are three of the same standards measured a year earlier. The green curve is a fit to the loglog of the new (blue) data in μm . The fitted parameters are $(a, x_0) = (-0.086, 2.60)$, of the function $a(x - x_0)^2$.

Since oblates dominate the measured samples, we will focus our model on those, instead of also considering prolates (section 3.3). As previously mentioned (section 2.3), oblate particles in a shear flow orient themselves with the flat side along the flow lines, while they are randomly oriented in the shear direction (Jeffery, 1922). Since they are free to rotate along an axis orthogonal to the light beam direction, we can model them as rectangles embedded in 2 dimensions for which all orientation angles are equally likely (supplement D). The light and detector also lie in the plane. In this 2 D model, d_{vol} is the square root of the area of the rectangle, and d_{ext} is the cross section of the rectangle.

Denoting the length of the short side b , the length the long side a , and the aspect ratio $c = b/a$, the probability of d_{ext} given a certain d_{vol} is

$$\frac{dP(d_{\text{ext}}|d_{\text{vol}})}{d \ln d_{\text{ext}}} = \begin{cases} 0 & \text{for } d_{\text{ext}} < b \\ z & \text{for } b < d_{\text{ext}} < a \\ 2z & \text{for } a < d_{\text{ext}} < \sqrt{a^2 + b^2} \end{cases}, \quad (1)$$

10 for

$$z = \frac{2}{\pi} \frac{1}{\sqrt{\frac{a^2 + b^2}{d_{\text{ext}}^2} - 1}}. \quad (2)$$

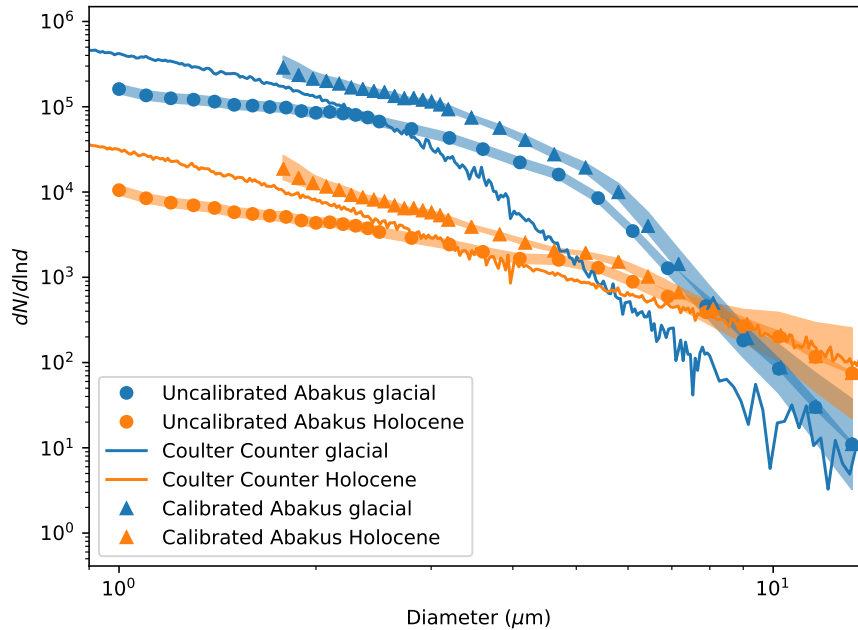


Figure 5. Size distribution of the dust particles in the RECAP ice core for both Holocene and last glacial period measured by Abakus and Coulter Counter. The y -axis is the probability density function of the particle number with respect to the logarithm of the diameter. The shaded areas represent the measurement uncertainty (supplement E). The calibrated Abakus data are calibrated using the fitted function from figure 4. The aspect ratio simulation is not included. The shaded areas around the calibrated data represent only the uncertainty from the calibration. For the Abakus, the diameter is extinction diameter, and for the Coulter Counter it is volumetric diameter.

The distribution of d_{ext} for all d_{vol} can then be found as

$$\frac{dP(d_{\text{ext}})}{d \ln d_{\text{ext}}} = \int \frac{dP(d_{\text{ext}}|d_{\text{vol}})}{d \ln d_{\text{ext}}} \frac{dP(d_{\text{vol}})}{d \ln d_{\text{vol}}} d \ln d_{\text{vol}}. \quad (3)$$

In section 3.2 we calibrated the Abakus such that $d_{\text{meas}} = d_{\text{ext}}$. Therefore $\frac{dP(d_{\text{ext}})}{d \ln d_{\text{ext}}}$ calculated here simulates Abakus measurements.

- 5 This can be used to find the aspect ratio of the particles just from the Coulter Counter-Abakus discrepancy. To do this, the sum of the square of the logarithm of the ratio between $\frac{dP(d_{\text{ext}})}{d \ln d_{\text{ext}}}$ calculated from the Coulter Counter data and the Abakus data was minimized with respect to the aspect ratio. This gives the aspect ratio where $\frac{dP(d_{\text{ext}})}{d \ln d_{\text{ext}}}$ is most consistent with the Abakus data, which is the most likely aspect ratio given the data. For the Holocene data this gave $c = 0.41 \pm 0.09$, while for the glacial $c = 0.31 \pm 0.04$. The errors are propagated from the total errors on the calibrated Abakus data. There is however a large
- 10 correlation between the errors on the Holocene and glacial data, so the error on the difference is only around 0.02, confirming a significant difference in aspect ratio between glacial and Holocene dust particles.

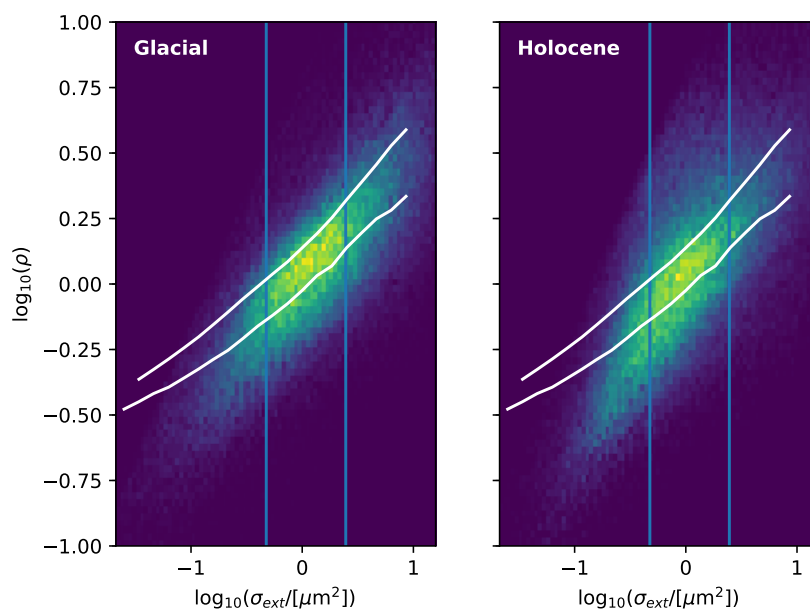


Figure 6. Glacial and Holocene samples measured by SPES. The brighter colors have a higher number of measured particles in a bin. The blue lines mark the 0.25 and 0.75 quantiles of σ_{ext} . The white curves are the mean optical thickness as a function of σ_{ext} for ADDA simulations with a refractive index of 1.55. The upper is for an aspect ratio of 0.5, the lower for 0.2.

4 Discussion

When the Abakus is calibrated using the true diameter of polystyrene spheres, it gives up to 10 times as many counts as the Coulter Counter for ice core samples (Figure 7). The discrepancy between the two instruments is systematic and exists because they measure two different properties of the particles, volume and extinction cross section. It is therefore not possible in general to calibrate the Abakus such that it yields the same distribution as the Coulter Counter for all ice core samples. However, by combining Coulter Counter and Abakus data, additional information is gained about the aspect ratio that was not available from the two instruments individually.

It has previously been suggested that it is impossible to calibrate the Abakus using polystyrene beads due to the strong Mie wiggles (Ruth, 2002, p. 20). It was argued that since for spheres the measured extinction cross section is a non-monotonous function of the true diameter, it cannot be inverted. However, this is based on the criterion that d_{meas} of the Abakus should be identical to d_{true} when measuring spheres. Since spheres have strong Mie wiggles but ice core dust does not, this criterion is invalid. Therefore the Abakus should be calibrated such that d_{meas} is equal to d_{ext} instead of d_{true} (section 3.2).

With the SPES instrument we found that the average aspect ratio of our ice core dust samples is 0.39 ± 0.03 for the Holocene and 0.33 ± 0.04 for the glacial, so the particles are significantly elongated (section 3.3). Using our simple model for the relation

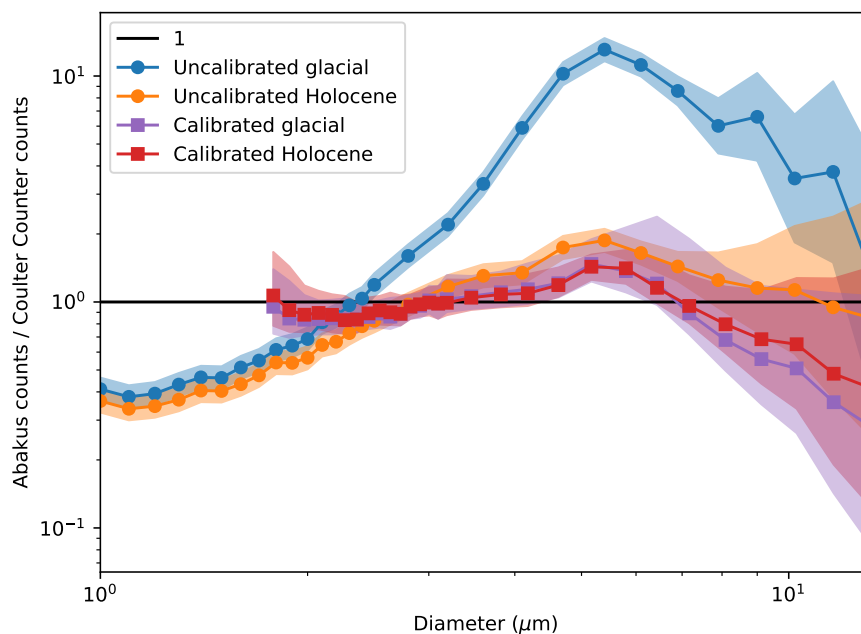


Figure 7. The circles represent the ratio between the uncalibrated Abakus and Coulter Counter data from figure 5, where the diameter is the measured diameter from the Abakus. The squares represent the ratio between the calibrated measured and modelled Abakus data, as described in section 3.4, where the diameter is the extinction diameter.

between d_{meas} and d_{vol} , we have calculated the aspect ratio independently from the Abakus and Coulter Counter data. This gave an aspect ratio of 0.41 ± 0.09 for the Holocene and 0.31 ± 0.04 for the glacial in accordance with SPES. In addition to giving the same aspect ratio as SPES, the model also gives a consistent size distribution within the Abakus uncertainties (Figure 7).

- 5 In the Dome C ice core from the East Antarctic plateau the aspect ratios of oblate and prolate particles have been determined to be 0.2 ± 0.1 and 3.5 ± 1.3 , respectively (Potenza et al., 2016). The ranges refer to the variability in the aspect ratio among different particles and not the uncertainty on the mean. In the RECAP ice core studied here, we found a similar but slightly less extreme aspect ratio both in the Holocene and in the glacial ice. For the RECAP core, we speculate that the Holocene dust originates from local Eastern Greenlandic sources, while the glacial dust is from central Asia (Bory et al., 2003). In Dome
- 10 C the dust is primarily attributed to southern South America (Delmonte et al., 2010). Measurements of dust particles in dust storms generally show an aspect ratio above 0.5. However, during transport, the dust fractionates towards more extreme aspect ratios (Knippertz and Stuut, 2014, p. 28-30). Since the large ice sheets are located far away from typical dust sources, the dust extracted from ice cores would be subject to more fractionation. Therefore we do expect more extreme aspect ratios to be found in ice core dust than in the atmospheric dust storm measurements. The greater aspect ratio of the local Greenlandic Holocene
- 15 dust compared to the Asian glacial dust agrees well with the observed aspect ratio fractionation observed in the atmosphere.



5 Conclusions

The Abakus laser sensor and the Coulter Coulter give different size distributions when measuring the same ice core dust sample. This is because ice core dust particles are not spherical, so the particle volume measurements of the Coulter Counter are different from the cross section measurements of the Abakus. When spherical particles are measured by the Abakus, the measured extinction diameter oscillates strongly as a function of particle size due to Mie scattering wiggles. The extinction diameter of ice core dust does not show these wiggles, but is proportional to the volumetric diameter. When the Abakus is calibrated using spherical particles, it should therefore be calibrated to the extinction diameter and not the true diameter.

We derived a model for extracting the aspect ratio of the dust particles from the differences between Abakus and Coulter Counter measurements of the same ice core dust samples. This process suggests an aspect ratio of 0.41 ± 0.01 for Holocene and 0.32 ± 0.01 for glacial dust samples from the RECAP ice core, consistent with direct aspect ratio measurements from a Single Particle Extinction and Scattering instrument. This shows that not only is the discrepancy between the two instruments explained by the non-spherical shape of the particles, it can also be used to obtain the aspect ratio. Moreover, by knowing the aspect ratio, a better size distribution can be obtained from the Abakus data.

6 Data availability

The data for all plots will be made available on www.iceandclimate.dk/data upon acceptance.



Appendix A: Bags measured by the Coulter Counter

Holocene				
bag	top depth (m)	bottom depth (m)	top age (years b2k)	bottom age (years b2k)
300	164.45	165.00	356	358
304	166.65	167.20	363	365
305	167.20	167.75	365	367
321	176.00	176.55	395	397
335	183.70	184.25	423	425
714	392.15	392.70	1980	1989
716	393.25	393.80	1998	2006
746	409.75	410.30	2282	2293
747	410.30	410.85	2293	2303
755	414.70	415.25	2379	2390
759	416.90	417.45	2423	2434
760	417.45	418.00	2434	2446
762	418.55	419.10	2457	2469
788	432.85	433.40	2785	2799
795	436.70	437.25	2884	2899
797	437.80	438.35	2914	2928
799	438.90	439.45	2943	2958
800	439.45	440.00	2958	2974
836	459.25	459.80	3588	3608
837	459.80	460.35	3608	3629
838	460.35	460.90	3629	3650
840	461.45	462.00	3671	3692
842	462.55	463.10	3713	3734
847	465.30	465.85	3822	3845
848	465.85	466.40	3845	3868
850	466.95	467.50	3890	3914
851	467.50	468.05	3914	3937
852	468.05	468.60	3937	3961
854	469.15	469.70	3984	4008



glacial					
bag	top depth (m)	bottom depth (m)	top age (years b2k)	bottom age (years b2k)	
972	534.05	534.60	17760	21170	
973	534.60	535.15	21170	24745	
974	535.15	535.70	24745	28783	
975	535.70	536.25	28783	33885	

Appendix B: Polystyrene sphere standards

The polystyrene sphere standards were produced by BS-Partikel GmbH, Wiesbaden, Germany. d_{true} is the certified diameter given by the manufacturer, d_{meas} is the diameter measured by the Abakus, and σ_{true} and σ_{meas} are their uncertainties.

Nominal diameter (μm)	d_{true} (μm)	d_{meas} (μm)	σ_{true} (μm)	σ_{meas} (μm)	Lot No.	Catalog No.
1.5	1.45	1.08	0.04	0.05	LS0248.161	LS0150-05
2	1.97	2.06	0.06	0.05	LS239.111	LS0200-05
4	3.77	3.12	0.14	0.27	LS237.161	LS0400-05
5	4.92	4.96	0.06	0.35	LS122.111	LS0500-05
10	10.37	10.83	0.14	0.71	LS108.509	LS1000-05

Appendix C: Microscope photographs

Photographs of both glacial and Holocene dust were taken through a microscope (Figures 8 and 9). The highly non-spherical shape is clearly seen. As the particles orient themselves with as low center of mass as possible on the substrate, they will typically lie on their flattest side. The aspect ratio is therefore not directly visible.

10 Appendix D: Extinction diameter calculation in the 2D model

The particles in the Abakus are modelled as 2D rectangles, for which all rotation angles are equally likely (Figure 10). The cross section of the particle is equal to d_{ext} in the 2D model.

D1 Rod

For calculating the cross section of a rectangle, the cross section of a rod is needed. We define a rod with length l and zero width. For an angle of rotation ϕ , the cross section is $d_{\text{ext}} = l \sin \phi$. From symmetry, the ϕ values are confined to $\phi \in [0, \frac{\pi}{2}]$. Assuming a uniform probability distribution for the angle, the probability of measuring the particle in the interval $[\phi, \phi + d\phi]$ is $dP(\phi; d\phi) = \frac{2}{\pi} d\phi$, which is normally written $\frac{dP(\phi)}{d\phi} = \frac{2}{\pi}$.

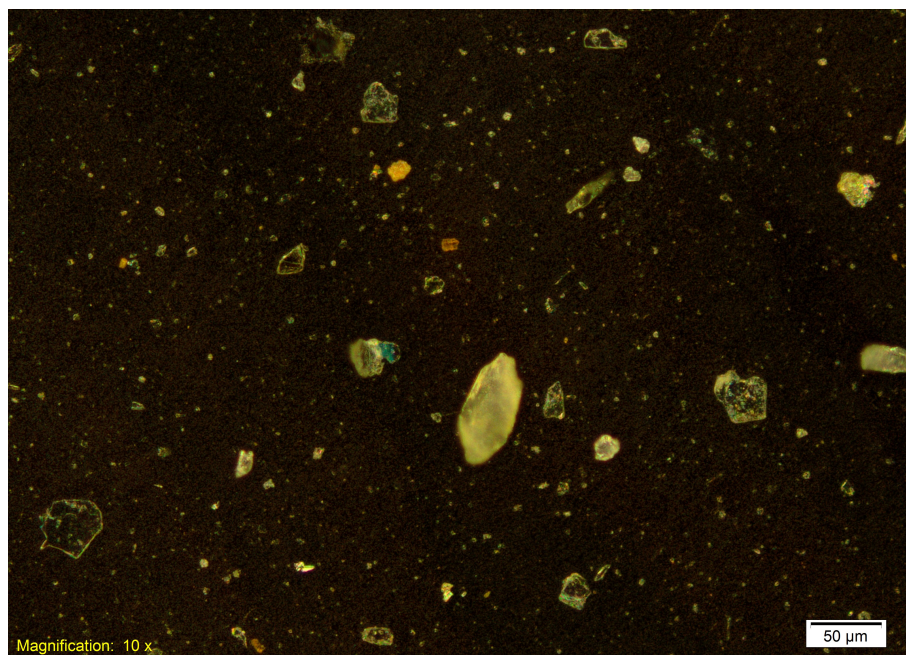


Figure 8. Microscope photograph of RECAP Holocene dust from bag 837.

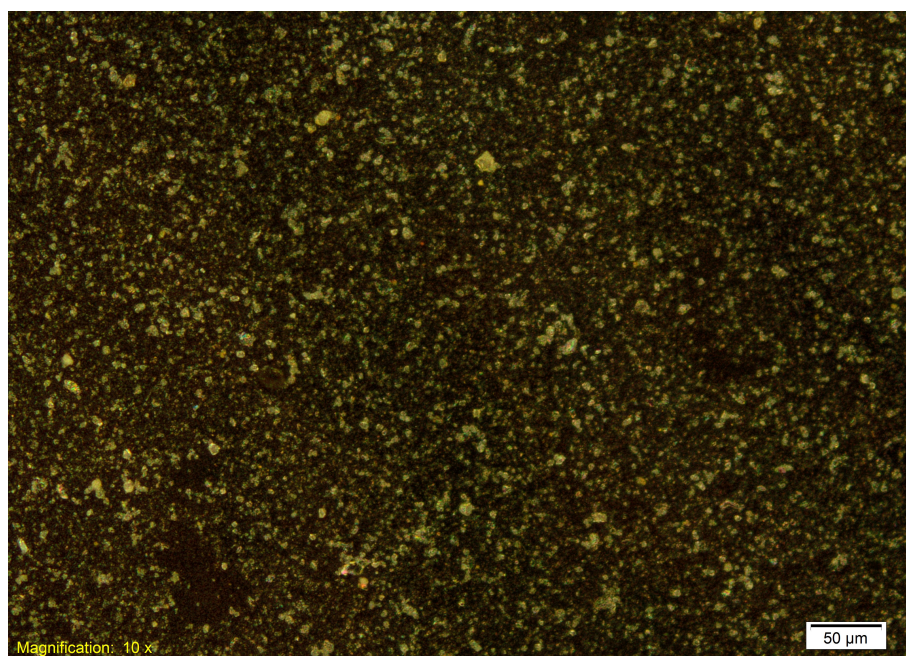


Figure 9. Microscope photograph of RECAP glacial dust from bag 975.

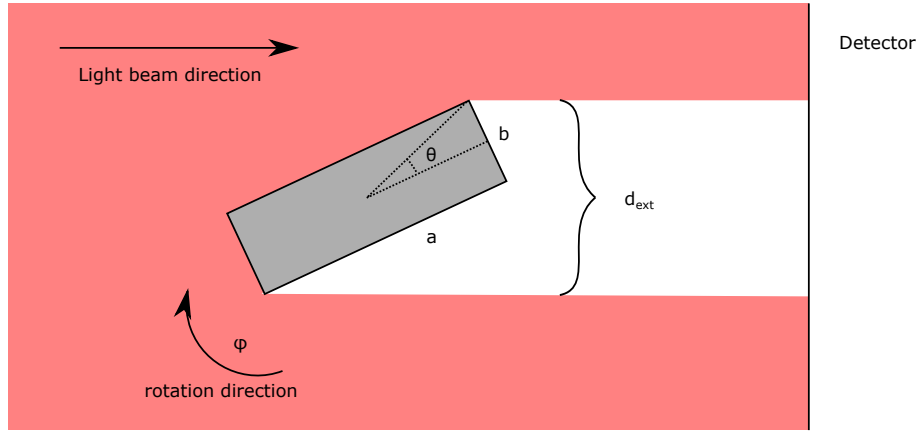


Figure 10. 2D model of the particle orientation in the Abakus.

For converting this to d_{ext} space, $d\phi$ needs to be expressed in terms of dd_{ext} :

$$d_{\text{ext}} = l \sin \phi \quad (\text{D1})$$

$$\Rightarrow dd_{\text{ext}} = l \cos \phi d\phi \quad (\text{D2})$$

$$\Rightarrow d\phi = \frac{1}{\sqrt{l^2 - d_{\text{ext}}^2}} dd_{\text{ext}} \quad (\text{D3})$$

5 Therefore

$$\frac{dP(d_{\text{ext}})}{dd_{\text{ext}}} = \frac{2}{\pi} \frac{1}{\sqrt{l^2 - d_{\text{ext}}^2}} \quad (\text{D4})$$

$$\Rightarrow \frac{dP(d_{\text{ext}})}{d \ln d_{\text{ext}}} = z, \quad (\text{D5})$$

where

$$z = \frac{2}{\pi} \frac{1}{\sqrt{\left(\frac{l}{d_{\text{ext}}}\right)^2 - 1}}. \quad (\text{D6})$$

- 10 It is seen that it diverges for $d_{\text{ext}} \rightarrow l$, because d_{ext} is almost constant as a function of angle when the rod is close to being perpendicular to the light source.

D2 Rectangle

Consider a rectangle with side lengths a and b . As for the rod, by symmetry, it is only necessary to consider the angles $\phi \in [0, \frac{\pi}{2}]$. In this case the cross section is given by the cross section of the diagonal. This is just the cross section of a rod rotated by

$$15 \quad \phi_+ = \phi + \theta \quad (\text{D7})$$

$$\Rightarrow \phi_+ \in [\theta, \frac{\pi}{2} + \theta], \quad (\text{D8})$$



where θ is the angle between the side a and the diagonal. If ϕ is uniformly distributed in $[0, \frac{\pi}{2}]$, so is ϕ_+ in $[\theta, \frac{\pi}{2} + \theta]$. The derivation for the rod is only valid when d_{ext} is a monotonous function of ϕ . This means that it can only be directly applied for $\phi_+ < \frac{\pi}{2}$. However, due to symmetry, the cross section is the same for $\phi_+ = \frac{\pi}{2} + \Delta\phi$ and $\phi_+ = \frac{\pi}{2} - \Delta\phi$, for any $\Delta\phi$. Therefore, the probability of measuring a cross section corresponding to $\phi \in [\frac{\pi}{2} - \theta, \frac{\pi}{2}]$ is twice as high as the probability of measuring the cross section of a rod in this interval. The cross section of $\frac{\pi}{2} - \theta$ is a . This means that the probability distribution is

$$\frac{dP(d_{\text{ext}})}{d \ln d_{\text{ext}}} = \begin{cases} 0 & \text{for } d_{\text{ext}} < b \\ z & \text{for } b < d_{\text{ext}} < a \\ 2z & \text{for } a < d_{\text{ext}} < \sqrt{a^2 + b^2} \end{cases}, \quad (\text{D9})$$

for

$$z = \frac{2}{\pi} \frac{1}{\sqrt{\frac{a^2 + b^2}{d_{\text{ext}}^2} - 1}}. \quad (\text{D10})$$

Appendix E: Replicate ice core measurements

The upper 93 m of the RECAP ice core has been measured twice (Figure 11). This means that two parallel sticks have been cut from the core, each of which has been measured on the Copenhagen CFA system. The CFA system was modified slightly between the two measurement campaigns, including changes in the pump and tubing setup, as well as general wear and roughening of the tubing walls. Therefore, the difference between the two measurements most likely reflects the error introduced by the CFA system. For the smaller particles, the replicate values are 12 % larger than the main. In comparison, for the large particles the replicate measurement has up to 3 times lower values than the main measurement. This is probably because the transport of the large particles from the melt head to the instrument depends more on the specific system setup than the small particle transport.

The difference between the two measurements is used as uncertainty for the Abakus measurements. However, a minimum uncertainty of 12 % is used, since the crossing of the two curves gives an artificially low difference.

Competing interests. The authors declare that they have no conflict of interest.

Acknowledgements. The RECAP ice coring effort was financed by the Danish Research Council through a Sapere Aude grant, the NSF through the Division of Polar Programs, the Alfred Wegener Institute, and the European Research Council under the European Community's Seventh Framework Programme (FP7/2007-2013) / ERC grant agreement 610055 through the Ice2Ice project. The Centre for Ice and Climate is funded by the Danish National Research Foundation.

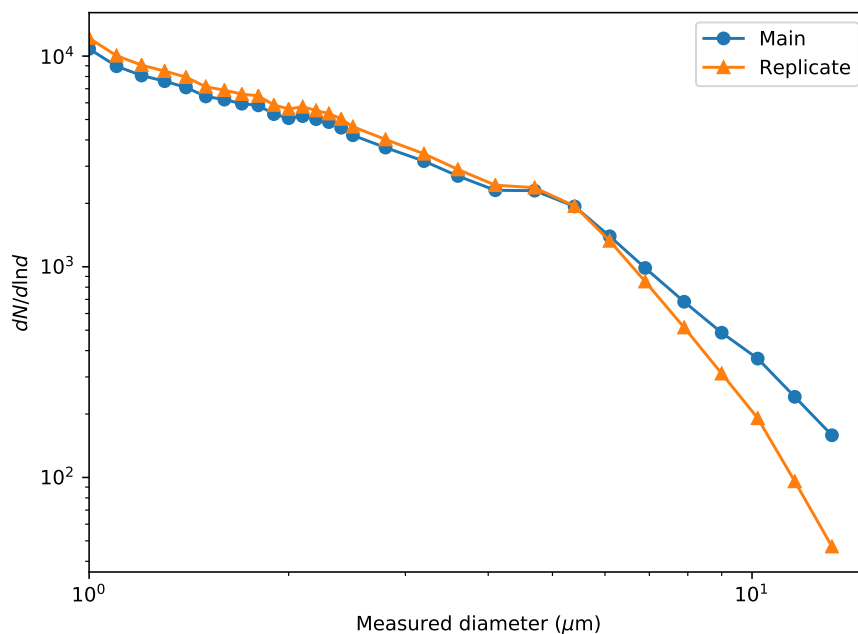


Figure 11. The upper 93 m of the RECAP ice core measured twice with the Abakus.

References

- Bigler, M., Svensson, A., Kettner, E., Vallelonga, P., Nielsen, M. E., and Steffensen, J. P.: Optimization of high-resolution continuous flow analysis for transient climate signals in ice cores, *Environmental science & technology*, 45, 4483–4489, 2011.
- Biscaye, P., Grousset, F., Revel, M., Van der Gaast, S., Zielinski, G., Vaars, A., and Kukla, G.: Asian provenance of glacial dust (stage 2) in the Greenland Ice Sheet Project 2 ice core, Summit, Greenland, *Journal of Geophysical Research: Oceans*, 102, 26 765–26 781, 1997.
- 5 Bory, A. J.-M., Biscaye, P. E., Piotrowski, A. M., and Steffensen, J. P.: Regional variability of ice core dust composition and provenance in Greenland, *Geochemistry, Geophysics, Geosystems*, 4, doi:10.1029/2003GC000627, <http://dx.doi.org/10.1029/2003GC000627>, 1107, 2003.
- Brazitikos, S., Giannopoulos, A., Valettas, P., and Vritsiou, B.: *Geometry of Isotropic Convex Bodies*, *Mathematical Surveys and Monographs*, American Mathematical Society, <https://books.google.dk/books?id=HmFsAwAAQBAJ>, 2014.
- 10 Chýlek, P. and Klett, J. D.: Extinction cross sections of nonspherical particles in the anomalous diffraction approximation, *JOSA A*, 8, 274–281, 1991.
- Delmonte, B., Petit, J., Andersen, K. K., Basile-Doelsch, I., Maggi, V., and Lipenkov, V. Y.: Dust size evidence for opposite regional atmospheric circulation changes over east Antarctica during the last climatic transition, *Climate Dynamics*, 23, 427–438, 2004.
- 15 Delmonte, B., Andersson, P., Schöberg, H., Hansson, M., Petit, J., Delmas, R., Gaiero, D., Maggi, V., and Frezzotti, M.: Geographic provenance of aeolian dust in East Antarctica during Pleistocene glaciations: preliminary results from Talos Dome and comparison with East Antarctic and new Andean ice core data, *Quaternary Science Reviews*, 29, 256–264, 2010.
- Draine, B. T. and Flatau, P. J.: Discrete-dipole approximation for scattering calculations, *JOSA A*, 11, 1491–1499, 1994.



- Hansson, M. E.: The Renland ice core. A Northern Hemisphere record of aerosol composition over 120,000 years, *Tellus B*, 46, 390–418, 1994.
- Jeffery, G. B.: The motion of ellipsoidal particles immersed in a viscous fluid, in: *Proceedings of the royal society of London A: Mathematical, physical and engineering sciences*, 715, pp. 161–179, The Royal Society, 1922.
- 5 Kaufmann, P. R., Federer, U., Hutterli, M. A., Bigler, M., Schüpbach, S., Ruth, U., Schmitt, J., and Stocker, T. F.: An improved continuous flow analysis system for high-resolution field measurements on ice cores, *Environmental science & technology*, 42, 8044–8050, 2008.
- Knippertz, P. and Stuu, J.-B. W.: On Composition, Morphology, and Size Distribution of Airborn Mineral Dust, in: *Mineral Dust*, pp. 15–50, Springer, 2014.
- Koffman, B. G., Kreutz, K., Breton, D., Kane, E., Winski, D., Birkel, S., Kurbatov, A., and Handley, M.: Centennial-scale variability of the
10 Southern Hemisphere westerly wind belt in the eastern Pacific over the past two millennia, *Climate of the Past*, 10, 1125–1144, 2014.
- Lambert, F., Delmonte, B., Petit, J. R., Bigler, M., Kaufmann, P. R., Hutterli, M. A., Stocker, T. F., Ruth, U., Steffensen, J. P., and Maggi, V.: Dust-climate couplings over the past 800,000[thins]years from the EPICA Dome C ice core, *Nature*, 452, 616–619, <http://dx.doi.org/10.1038/nature06763>, 2008.
- Lambert, F., Bigler, M., Steffensen, J. P., Hutterli, M., and Fischer, H.: Centennial mineral dust variability in high-resolution ice core data
15 from Dome C, Antarctica, *Climate of the Past*, 8, 609–623, doi:10.5194/cp-8-609-2012, <https://www.clim-past.net/8/609/2012/>, 2012.
- Potenza, M. A. C., Albani, S., Delmonte, B., Villa, S., Sanvito, T., Paroli, B., Pullia, A., Baccolo, G., Mahowald, N., and Maggi, V.: Shape and size constraints on dust optical properties from the Dome C ice core, Antarctica, *Scientific Reports*, 6, 28 162 EP –, <http://dx.doi.org/10.1038/srep28162>, 2016.
- Röthlisberger, R., Bigler, M., Hutterli, M., Sommer, S., Stauffer, B., Junghans, H. G., and Wagenbach, D.: Technique for continuous high-
20 resolution analysis of trace substances in firn and ice cores, *Environmental Science & Technology*, 34, 338–342, 2000.
- Royer, A., De Angelis, M., and Petit, J.: A 30000 year record of physical and optical properties of microparticles from an East Antarctic ice core and implications for paleoclimate reconstruction models, *Climatic Change*, 5, 381–412, 1983.
- Ruth, U.: Concentration and size distribution of microparticles in the NGRIP ice core (Central Greenland) during the last glacial period, Ph.D. thesis, University of Bremen, 2002.
- 25 Ruth, U., Wagenbach, D., Steffensen, J. P., and Bigler, M.: Continuous record of microparticle concentration and size distribution in the central Greenland NGRIP ice core during the last glacial period, *Journal of Geophysical Research: Atmospheres*, 108, 2003.
- Saey, P.: Diplomarbeit im Studiengang Physik, Master’s thesis, Fakultät für Physik und Astronomie, Ruprecht-Karls-Universität Heidelberg, 1998.
- Steffensen, J. P.: The size distribution of microparticles from selected segments of the Greenland Ice Core Project ice core representing
30 different climatic periods, *Journal of Geophysical Research: Oceans*, 102, 26 755–26 763, 1997.
- van de Hulst, H. C.: *Light scattering by small particles*, Courier Corporation, 1957.
- Villa, S., Sanvito, T., Paroli, B., Pullia, A., Delmonte, B., and Potenza, M. A. C.: Measuring shape and size of micrometric particles from the analysis of the forward scattered field, *Journal of Applied Physics*, 119, 224 901, doi:10.1063/1.4953332, <http://dx.doi.org/10.1063/1.4953332>, 2016.
- 35 Yurkin, M. A. and Hoekstra, A. G.: The discrete-dipole-approximation code ADDA: capabilities and known limitations, *Journal of Quantitative Spectroscopy and Radiative Transfer*, 112, 2234–2247, 2011.